The Design of the Speed Control System of Supercharger Using Microcontroller

Wiroj Khawlaor[1], Kittiya Nakphan[2], Phichitphon Chotikunnan[3*]

[1]*Energy and Logistics Engineering department, Faculty of Engineering and Technology, Siam Technology College, 46 Charansanitwong Road, Gate 2, Tha Phra Sub-district, Bang Kho Laem District, Bangkok 10600, Thailand; E-mail: wirojk@siamtechno.ac.th*

[2]*Occupational Health and Safety Department, Faculty of Health Sciences, Siam Technology College, 46 Charansanitwong Road, Gate 2, Tha Phra Sub-district, Bang Kho Laem District, Bangkok 10600, Thailand; E-mail: kittiyan@siamtechno.ac.th*

[3]*College of Biomedical Engineering, Rangsit University, Pathum Thani, Thailand 12000; E-mail: phichitphon.c@rsu.ac.th*

Abstracts: The cruise control system regulates the car's speed, focusing on simulating and assessing the air compressor's speed control within the engine speed control system. Comprising a microcontroller PIC30 main board, H-Bridge DC motor drive board, encoder, 12V DC motor, supercharger, and PC interface with MATLAB and Simulink, the system aims for efficient speed control. Simulation results showcase the impact on DC electric motor speed control, emphasizing clarity and stability. The study outlines distinct outcomes: 1) Deactivation of the control system. 2) Activation at 1100 rpm. 3) Operation at 1200 rpm. 4) Functioning at 1400 rpm. Observations reveal that without the air compressor, the system struggles to control rotational speed. Conversely, with the control system engaged, consistent average errors of 0.63% occur across the three specified speeds. The setting time remains under 2 seconds. Subsequently, the control system autonomously readjusts the speed to the predefined specifications. The research highlights the system's effectiveness in achieving stable speed control, offering insights into its practical application within automotive engineering.

Keywords: Rise Time, Setting Time, Speed Control, PID Controller.

1. INTRODUCTION

In the continuously evolving realm of vehicle technology, progress encompasses both traditional engine-driven propulsion systems and electric propulsion systems. The central aim of these technological advancements is to enhance human life by providing sustainable and comfortable transportation solutions. Despite these strides, a persistent challenge during extended journeys is driver fatigue. This issue has prompted significant attention from researchers toward vehicle speed control systems, particularly cruise control systems, which operate automatically to maintain a consistent speed and alleviate driver fatigue, especially during long-distance travel.

This study emphasizes the importance of integrating cruise control systems with adaptive cruise control mechanisms. The objective is to ensure a steady speed, even in the face of external factors such as varying road conditions or defensive maneuvers. The application of this technology extends to various fields, notably in automotive engineering. The research introduces a cruise control system coupled with an adaptive cruise control system tailored for air compressors. This system is specifically designed to regulate the rotational speed of the engine. By incorporating this system into the air compressor, an integral component of the engine control system in conventional vehicles, maintaining a constant engine speed becomes attainable [1]-[2]. The control process is divided into two loops: the inner loop manages the current, while the outer loop governs the engine speed using a cascaded control structure. This sequential arrangement of control loops enhances system efficiency.

Motivated by these principles, the research team applies the cruise control system to an air compressor, showcasing its capability to maintain a consistent rotational speed. The integration of this technology holds promise for the broader automotive industry, ensuring improved engine performance and efficiency by effectively controlling the air compressor's speed. This study lays the foundation for the implementation of cruise control systems in

various applications, contributing to the ongoing advancement of automotive engineering.

Furthermore, in the quest to enhance motor efficiency, diverse control systems, such as PID Control [3]-[17] and fuzzy logic control [18]-[24], have been employed. Recent developments include innovative algorithms like the enhanced artificial transgender longicorn algorithm and recurrent neural networks [25] for stabilizing brushless DC (BLDC) motors.

In this research, the presentation of “The design of the speed control system of supercharger using microcontroller” highlights the utilization of PID Control [26]-[38] to regulate the motor's rotation in the speed control system of the supercharger. The study specifically designs a PI Controller under different rotational conditions, contributing to a broader understanding of control systems in diverse motor control applications.

2. MATERIEL AND METHODS

For the study, a segment focuses on the cruise control system of the air compressor to further integrate it into maintaining the constant speed of the engine or applying it to small-scale electricity-generating machines. This aims to ensure a consistent rotational speed when subjected to varying loads. The theoretical framework relevant to this study is explored, and the experimental apparatus employed in the testing phase is outlined.

2.1. PID Control System

The primary operating principle employed in automatic control systems is the PID control. This linear control operation stems from the summation in terms of the proportional error, integral of the error, and derivative of the error values. Based on this foundational concept, PID control has undergone extensive development, utilizing key variables such as the error value, output, which is the fundamental quantity indicating the difference between the actual and desired positions of the motor shaft. In this study, the focus is on investigating angular velocity control, presenting the equations used for approximating values in the control system. Equation (1) represents the system error, while Equation (2) denotes the equation for the PID controller.

$$e(t) = r(t) - y(t) \tag{1}$$

$$y(t) = K_p \,.\, e(t) + K_i \int_0^t e(t)dt + K_d \frac{d}{dt} e(t) \tag{2}$$

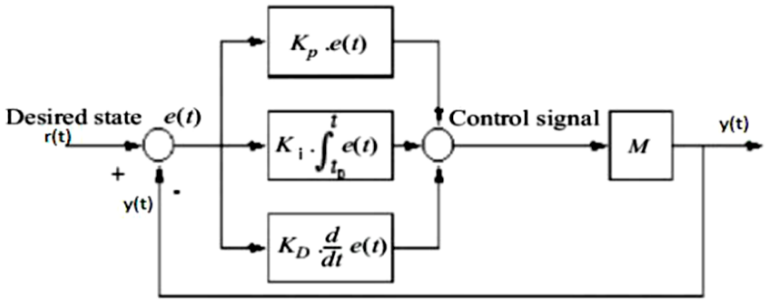

Figure 1. PID Controller's Block Diagram

In the diagram, where K_p, K_i, and K_d represent the proportional, integral, and derivative gains, respectively, as shown in Figure 1 depicting the control system block diagram. The process begins with the output of the system, *y(t)* (system output), being fed back and compared with the setpoint value, *r(t)* (system setpoint), at the summation point, resulting in the error signal *e(t).* The error signal is generated over time as follows: *e(t) = r(t) – y(t).* Subsequently, the PID loop acts to reduce the error value. The control signal *u(t)* is then sent to our system M for

regulating the response to meet the desired outcome. The system's output, *y(t),* is used in the subsequent loop to minimize the error value further.

2.2. DC Electric Motor

Controlling the rotational speed of the air compressor serves as a guideline for potential advancements in engine speed regulation. Figure 2 illustrates a crucial power transmission component, the 24V DC motor. Specifically, a 24V 500W 2500 rpm DC motor was selected to drive the air compressor, ensuring an adequate rotational speed conducive to engine operation. This choice aligns with the engine's operational speed of 3500 rpm, with the motor operating at 80% of the engine speed for compatibility with the control system design.

Figure 2. DC motor 24V 500W 2500 rpm

2.3. Motor H-Bridge Drive Board

The motor drive board, as depicted in Figure 3, is designed for driving the 24V DC electric motor. The chosen DC motor operates with a direct current, drawing a current of 25 Amps. Consequently, a motor drive board with a rating of 80 Amps was selected to accommodate the motor's power requirements.

Figure 3. Motor Drive Board for 24V 80A DC Electric Motor

2.4. Air Compressor AMR500

The air compressor can be classified into three main types. The reciprocating type can generate high compression force but has the drawback of producing pulsating flow. On the other hand, the centrifugal type provides low pressure, leading to the choice of a roots blower, which falls between the two types and maintains a continuous flow rate. The Roots blower's pressure is increased by the rotor's meshing, featuring two identical blade sets. One advantage is that the rotor meshing does not involve the use of oil, ensuring that the airflow remains uncontaminated. The air compressor is assembled with an electric motor to provide the driving force, as illustrated in Figure 4.

Figure 4. Air Compressor AMR500

2.5. Equipment Operation Structure

In designing the operational structure, as illustrated in Figure 5, the air compressor is directly connected to the 24V motor to minimize power losses in the drive system. This direct connection ensures that the rotational speed of the air compressor is equal to the motor's speed, facilitating convenient speed control.

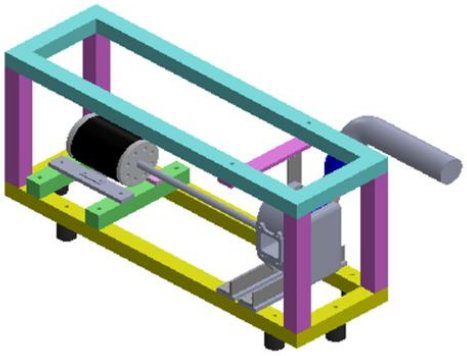

Figure 5. Design of the Speed Control System Structure

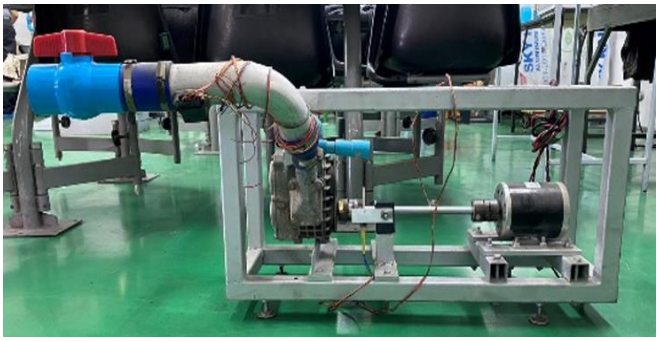

Figure 6. Practical Implementation of the Speed Control System Structure

Figure 6 illustrates the practical assembly of the speed control system. The framework is constructed using 1.5-inch steel boxes, serving as a base for mounting the motor and the air compressor.

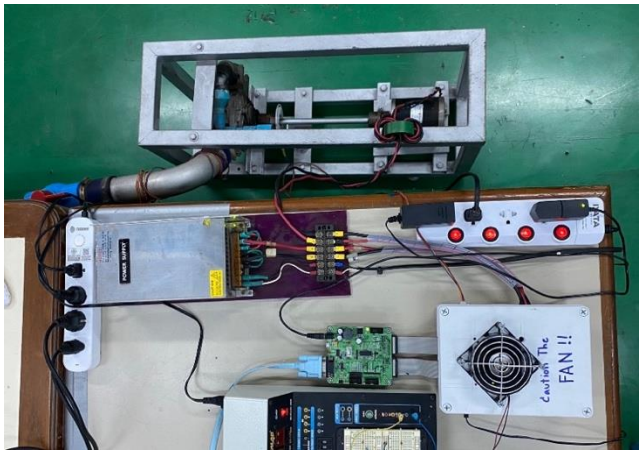

Figure 7. Structure of the Air Compressor Speed Control System

Figure 7 showcases the components used in controlling the rotational speed, comprising a pic30 control board, a 24V 80A motor drive board, a 24V power supply, the motor, the air compressor, and a Windows 7 or newer

computer. The pic30 control board communicates with the computer to exchange data, transmitting signals to the motor drive board for amplification, allowing it to drive the 24V motor. Consequently, the air compressor rotates according to the motor's rotational speed. The air compressor incorporates a photo sensor and an encoder to measure its rotational speed and the motor's speed. When the sensor receives signals, it transmits them to the pic30 control board, which processes the error value based on the pre-defined control program. The control signal is then sent to the plant, and the sensor receives the output signal for feedback to the controller. This process continues in a loop. The rotational speeds tested are 1100, 1200, and 1400, with the valve opened by 5 degrees to introduce a load to the system. The valve is alternately opened and closed to observe the control system's response under normal operation.

3. RESULTS AND DISCUSSIONS

In designing the PID controller system, the system gain values for the PI control were set as follows, K_p = 0.0005 and K_i = 0.0015. Through testing, the air compressor rotational speeds were divided into three values, 1100, 1200, and 1400 rpm. The system's control diagram is illustrated in Figure 8, with an output value of 1391 rpm fed back to the summing point for comparison with the desired state of 1400 rpm. The resulting error value is then forwarded to the controller. The controller works to minimize the error, sending the control signal to the motor through a constant gain slider. The system includes a manual switch for toggling between Manual and Automatic control modes.

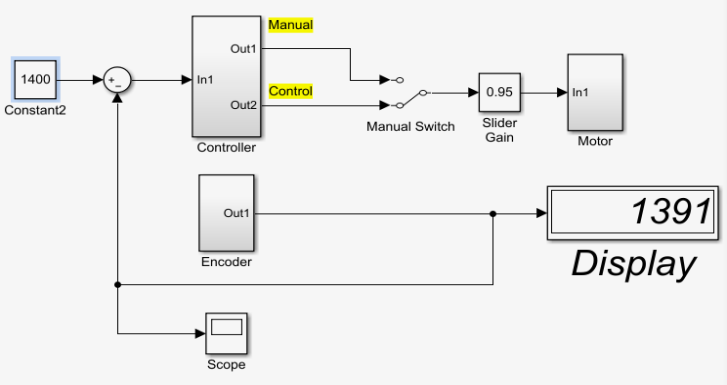

Figure 8. Overview of the Control System Diagram for Air Compressor Speed Control at 1400 RPM

The control system's performance was evaluated without activating the control system and without applying any load. The rotational speed was measured at 1010 RPM, as depicted in Figure 9. The figure illustrates the relationship between the air compressor's rotational speed (Y RPM) and time (X seconds). This data was obtained from the direct power of the DC motor (24V) without engaging the control system and without adding any load. It aims to demonstrate the idle speed of the motor, which can be set, with a value of 1010 RPM.

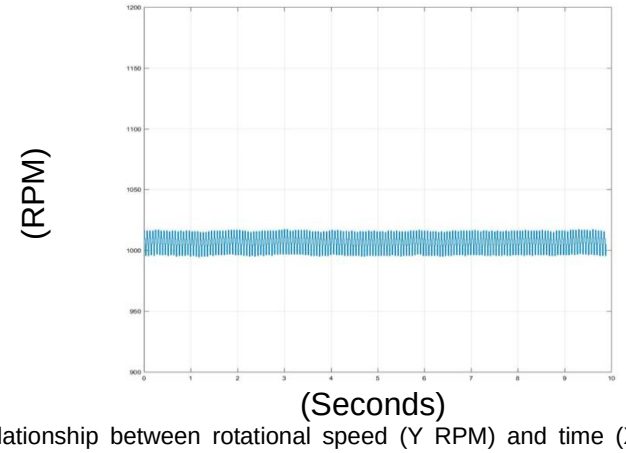

Figure 9. Displaying the relationship between rotational speed (Y RPM) and time (X seconds) while the control system is inactive and no load is applied. The rotational speed is maintained at 1010 RPM

From the control system results, with a rotational speed of 1075 RPM and the introduction of a load without activating the control system, as shown in Figure 10. The relationship begins with an idle speed of 1075 RPM (adjustable initial value). When the load is added at 2.1 seconds, the rotational speed decreases to 1050 RPM, and there is no further adjustment as the control system is not activated. Subsequently, releasing the load at 8.3 seconds shows that the rotational speed graph returns to the initial value of 1075 RPM, indicating the system's operation without automatic control activation.

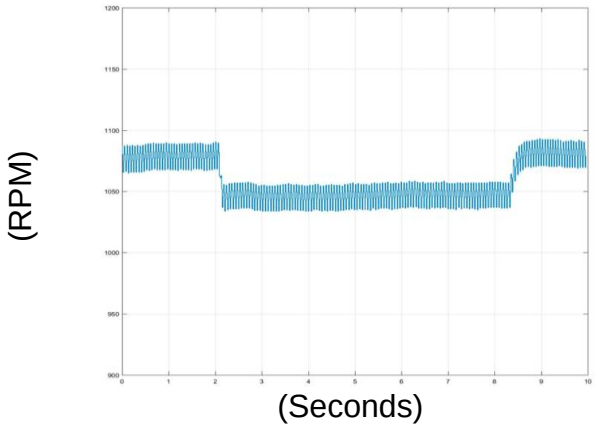

Figure 10. Displaying the relationship between rotational speed (Y RPM) and time (X seconds) at a rotational speed of 1075 RPM and adding a load to the system without activating the control system

The test results of the system at a rotational speed of 1100 RPM, with the addition of a load to the system and the control system activated, are shown in Figure 11. The graph illustrates the relationship between the rotational speed of the air compressor (RPM) and time. The system was initially set at a speed of 1100 RPM, and a load was applied at 2.3 seconds. The load was then held constant to observe the system's response. It was observed that when the system experienced the load (valve closed by 5 degrees), the system's speed dropped until reaching a minimum at 2.7 seconds. Afterward, the control system compensated for the value and increased the rotational speed until it returned to the initial steady state speed at 3.5 seconds. The load was then held at 5 degrees until 6.8 seconds, and upon releasing the load, the system's speed increased to 1150 RPM. The controller detected that it exceeded the set point of 1100 RPM and reduced the control signal to bring the system's speed back to the set steady state at 8.2 seconds, maintaining it thereafter. This graph illustrates the operation of the speed control system of the air compressor at the specified speed of 1100 RPM when the control system is activated.

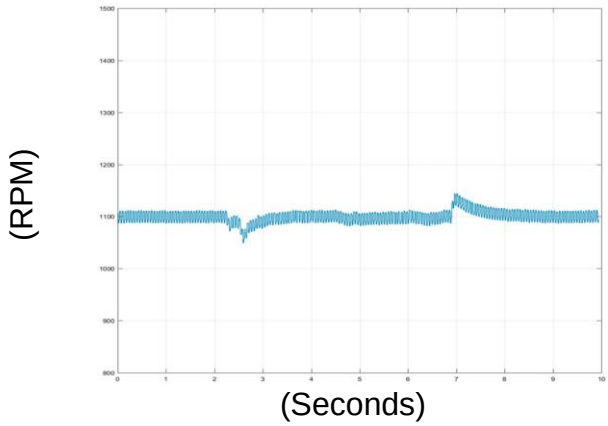

Figure 11. The relationship between the rotational speed (Y RPM) and time (X seconds) when the rotational speed is 1100 rpm, with an increase in load applied to the system by opening the control system

At a rotational speed of 1200 rpm, when applying a load to the system by opening the control system, the relationship between the rotational speed of the air compressor (rpm) and time is shown in Figure 12. The rotational speed is set to 1200 rpm, and a load is applied at 1.7 seconds. The load is held until 2.3 seconds to observe the

system's response. It is observed that when the system is loaded (valve closed by 5 degrees), the system's rotational speed drops until it reaches a minimum at 2.3 seconds. The control system then compensates and increases the rotational speed until it returns to the initial steady state speed at 3.5 seconds. The load is then held at 5 degrees until 7.2 seconds, after which the load is released. It is found that the system's rotational speed increases to 1242 rpm. The controller detects this deviation from the designed set point of 1200 rpm and reduces the control signal to bring the system's rotational speed back to the set steady state at 8.3 seconds, maintaining it thereafter. The graph illustrates the operation of the speed control system for the air compressor at the specified speed of 1200 rpm when the control system is activated. Notably, the graph reveals a disturbance around 7.5 seconds, attributed to encoder system malfunction, although the system continues to operate.

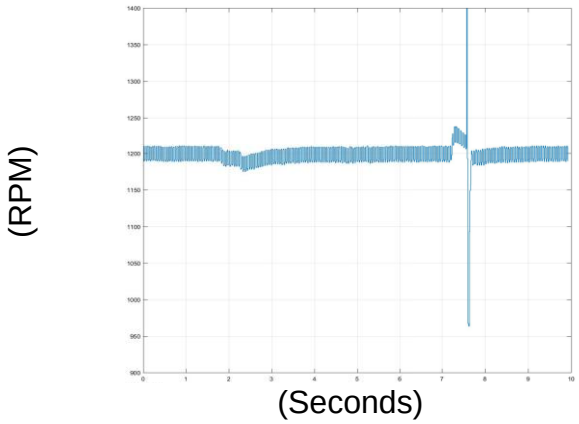

Figure 12. The relationship between the rotational speed (Y RPM) and time (X seconds) when increasing the load on the system by opening the control system, with the initial rotational speed set at 1200 rpm

At the speed of 1400 rpm, when applying a load to the system by opening the control system as shown in Figure 13, it demonstrates the relationship between the speed of the air compressor (rpm) versus time. The speed setting is configured at 1400 rpm, and a load is applied for a duration of 2.0 seconds, maintaining the load thereafter to observe the system's response. It is observed that when the system is subjected to a load (closing the valve by 5 degrees), the system speed decreases until reaching a minimum at 2.4 seconds. Subsequently, the control system compensates and increases the speed until returning to the initial speed at steady state at 3.9 seconds. The load is then held at 5 degrees until 7.7 seconds, at which point the load is released. It is found that the system speed increases to 1438 rpm, exceeding the designed set point of 1400 rpm. The control system detects this deviation and reduces the control signal to bring the system speed back to the set steady state value at 9.0 seconds, maintaining it thereafter. The graph illustrates the operation of the speed control system of the air compressor at the specified speed of 1400 rpm. The control system, when activated, effectively regulates the speed according to the designed set point, as summarized in Table 1.

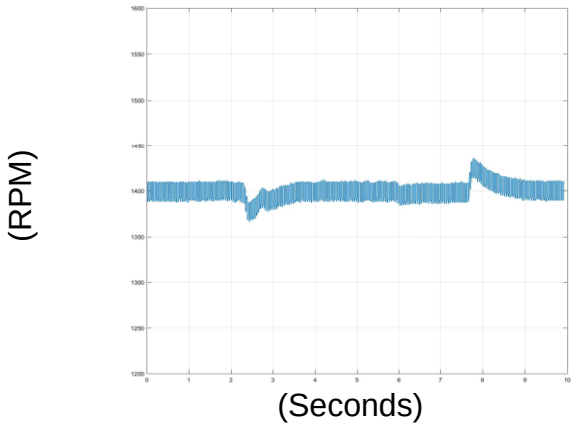

Figure 13. The relationship between the rotational speed (Y RPM) and time (X seconds) when the rotational speed is 1400 rpm, with an increase in load applied to the system, by opening the control system

Based on the test results in Table 1, it was found whether the control system operates as designed. It was observed that the control system operates as intended. When the system received a load at 2.3 seconds, it compensated for the speed reduction, resulting in a decrease to 1080 rpm. Subsequently, the system increased the speed until it reached the initial speed of 1100 rpm at 3.5 seconds.

Table 1. Display test results with specified speed

Test	1	2	3
Valve Opening Percentage	5%	5%	5%
Set Point [Speed of Motor (rpm)]	1100	1200	1400
Test Result (rpm)	1107	1192	1391
Error (%)	0.63	0.66	0.64

From the test results, it was observed that the speed control of the air compressor when the control system is not activated shows a correlation between the compressor speed and the load value. Increasing the load causes a decrease in compressor speed, and reducing the load results in an increase in compressor speed. When the automatic speed control system is activated, it was found that increasing the load leads to a decrease in compressor speed, taking approximately 2 seconds for the speed to decrease. Conversely, reducing the load causes an increase in compressor speed, reaching the designated design set point. The test was divided into three segments to assess the impact of increasing speed, and it was found that at a speed of 1100 rpm, the steady time is 1.2 seconds, at 1200 rpm it is 1.8 seconds, and at 1400 rpm it is 1.9 seconds. Calculating the performance coefficient yielded an average error value of 0.64%, as shown in Table 1.

CONCLUSIONS

In conclusion, the research findings demonstrate the effective performance of the PID controller system in regulating the speed of the air compressor. The designed control system, with specified parameters of Kp = 0.0005 and Ki = 0.0015, showcased commendable results across various test scenarios at rotational speeds of 1100, 1200, and 1400 rpm. The control system efficiently responded to changes in load, compensating for deviations and swiftly returning the compressor's rotational speed to the designated set points. The graphical representations of the system's response at different speeds and load conditions provided valuable insights into its dynamic behavior. Notably, the control system exhibited a remarkable average error value of 0.64%, underscoring its accuracy in maintaining the desired speeds. Furthermore, the study identified potential areas for improvement, particularly in addressing encoder system malfunctions that caused disturbances in the recorded data. Future enhancements could involve refining the precision of components such as encoders and employing higher-resolution microcontrollers for even more rapid and precise responses. In summary, the research affirms the efficacy of the designed PID controller system for air compressor speed control, paving the way for continued advancements and applications in diverse industrial settings.

Acknowledgments

The researcher would like to express gratitude to Siam Technology College for their generous support in providing research facilities and various equipment. Special thanks to the President, Assoc. Prof. Phoripat Mongkolvanich, for the opportunity to engage in diverse research endeavors, as well as for valuable guidance and assistance both academically and in research operations. Appreciation is extended to my mother, Thanatana, and brother, Surasit Khaolao, for their financial support in research endeavors. Thanks are also due to the staff of the Faculty of Engineering and Technology for their continuous support and facilitation in various aspects. Your kindness is truly appreciated.

REFERENCES

[1] M. Xiao, H. Zhu, Z. Du, Y. Gao, H. Tian, and G. Cai, “Design optimization of velocity-controlled cruise vehicle propelled by throttleable hybrid rocket motor,” Aerospace Science and Technology, vol. 115, p. 106784, 2021.

[2] H. Balaska, S. Ladaci, H. Schulte, and A. Djouambi, “Adaptive cruise control system for an electric vehicle using a fractional order model reference adaptive strategy,” IFAC-PapersOnLine, vol. 52, no. 13, pp. 194-199, 2019.

[3] I. Zaway, R. Jallouli-Khlif, B. Maaleja, H. Medhaffar, and N. Derbela, “Multi-objective Fractional Order PID Controller Optimization for Kid's Rehabilitation Exoskeleton,” International Journal of Robotics and Control Systems, vol. 3, no. 1, pp. 32-49, 2022. doi: 10.31763/ijrcs.v3i1.840.

[4] Z. Abdullah, S. Shneen, and H. Dakheel, “Simulation Model of PID Controller for DC Servo Motor at Variable and Constant Speed by Using MATLAB,” Journal of Robotics and Control (JRC), vol. 4, no. 1, pp. 54-59, 2023. doi: 10.18196/jrc.v4i1.15866.

[5] L. Thuy Anh, T. Thi Thanh Nga, and V. Van Hoc, “PID-Type Iterative Learning Control for Output Tracking Gearing Transmission Systems,” International Journal of Robotics and Control Systems, vol. 1, no. 3, pp. 256-268, 2021. doi: 10.31763/ijrcs.v1i3.395.

[6] M. Shamseldin and M. Abdelghany, “A New Self-Tuning Nonlinear PID Motion Control for One-Axis Servomechanism with Uncertainty Consideration,” Journal of Robotics and Control (JRC), vol. 4, no. 2, pp. 118-127, 2023. doi: 10.18196/jrc.v4i2.17433.

[7] C. Ben Jabeur and H. Seddik, “Optimized Neural Networks-PID Controller with Wind Rejection Strategy for a Quad-Rotor,” Journal of Robotics and Control (JRC), vol. 3, no. 1, pp. 62-72, 2021. doi: 10.18196/jrc.v3i1.11660.

[8] C. Márquez-Vera, Z. Yakoub, M. Márquez Vera, and A. Ma'arif, “Spiking PID Control Applied in the Van de Vusse Reaction,” International Journal of Robotics and Control Systems, vol. 1, no. 4, pp. 488-500, 2021. doi: 10.31763/ijrcs.v1i4.490.

[9] M. Shamseldin, “Adaptive Controller with PID, FOPID, and NPID Compensators for Tracking Control of Electric – Wind Vehicle,” Journal of Robotics and Control (JRC), vol. 3, no. 5, pp. 546-565, 2022. doi: 10.18196/jrc.v3i5.15855.

[10] Jam, F. A., Sheikh, R. A., Iqbal, H., Zaidi, B. H., Anis, Y., & Muzaffar, M. (2011). Combined effects of perception of politics and political skill on employee job outcomes. African Journal of Business Management, 5(23), 9896-9904.

[11] M. Elouni, H. Hamdi, B. Rabaoui, and N. Braiek, “Adaptive PID Fault-Tolerant Tracking Controller for Takagi-Sugeno Fuzzy Systems with Actuator Faults: Application to Single-Link Flexible Joint Robot,” International Journal of Robotics and Control Systems, vol. 2, no. 3, pp. 523-546, 2022. doi: 10.31763/ijrcs.v2i3.762.

[12] M. Iqbal and W. Aji, “Wall Following Control System with PID Control and Ultrasonic Sensor for KRAI 2018 Robot,” International Journal of Robotics and Control Systems, vol. 1, no. 1, pp. 1-14, 2021. doi: 10.31763/ijrcs.v1i1.206.

[13] D. Sonny Febriyan and R. Dwi Puriyanto, “Implementation of DC Motor PID Control On Conveyor for Separating Potato Seeds by Weight,” International Journal of Robotics and Control Systems, vol. 1, no. 1, pp. 15-26, 2021. doi: 10.31763/ijrcs.v1i1.221.

[14] H. Budiarto, V. Triwidyaningrum, F. Umam, and A. Dafid, “Implementation of Automatic DC Motor Braking PID Control System on (Disc Brakes),” Journal of Robotics and Control (JRC), vol. 4, no. 3, pp. 371-387, 2023. doi: 10.18196/jrc.v4i3.18505.

[15] M. Rabah, A. Rohan, and S. H. Kim, “Comparison of position control of a gyroscopic inverted pendulum using PID, fuzzy logic and fuzzy PID controllers,” International Journal of Fuzzy Logic and Intelligent Systems, vol. 18, no. 2, pp. 103–110, 2018, doi: 10.5391/IJFIS.2018.18.2.103.

[16] D. Tran, N. Hoang, N. Loc, Q. Truong, and N. Nha, “A Fuzzy LQR PID Control for a Two-Legged Wheel Robot with Uncertainties and Variant Height,” Journal of Robotics and Control (JRC), vol. 4, no. 5, pp. 612–620, 2023, doi: 10.18196/jrc.v4i5.19448.

[17] A. Latif, A. Zuhri Arfianto, H. Agus Widodo, R. Rahim, and E. T. Helmy, “Motor DC PID System Regulator for Mini Conveyor Drive Based-on Matlab,” Journal of Robotics and Control (JRC), vol. 1, no. 6, pp. 185-190, 2020, DOI: 10.18196/jrc.1636.

[18] P. Chotikunnan and R. Chotikunnan, “Dual Design PID Controller for Robotic Manipulator Application,” Journal of Robotics and Control (JRC), vol. 4, no. 1, pp. 23-34, 2023, doi: https://doi.org/10.18196/jrc.v4i1.16990.

[19] B. Panomruttanarug and P. Chotikunnan, “Self-balancing iBOT-like wheelchair based on type-1 and interval type-2 fuzzy control,” in 2014 11th International Conference on Electrical Engineering/Electronics, Computer, Telecommunications and Information Technology (ECTI-CON), May 2014, pp. 1-6, DOI: 10.1109/ECTICon.2014.6839710.

[20] P. Chotikunnan and B. Panomruttanarug, “The application of fuzzy logic control to balance a wheelchair,” Journal of Control Engineering and Applied Informatics, vol. 18, no. 3, pp. 41-51, 2016.

[21] P. Chotikunnan, R. Chotikunnan, A. Nirapai, A. Wongkamhang, P. Imura, and M. Sangworasil, “Optimizing Membership Function Tuning for Fuzzy Control of Robotic Manipulators Using PID-Driven Data Techniques,” Journal of Robotics and Control (JRC), vol. 4, no. 2, pp. 128-140, 2023, DOI: 10.18196/jrc.v4i2.18108.

[22] Jam, F., Donia, M., Raja, U., & Ling, C. (2017). A time-lagged study on the moderating role of overall satisfaction in perceived politics: Job outcomes relationships. Journal of Management & Organization, 23(3), 321-336. doi:10.1017/jmo.2016.13

[23] P. Chotikunnan, and Y. Pititheeraphab, “ Adaptive P Control and Adaptive Fuzzy Logic Controller with Expert System Implementation for Robotic Manipulator Application,” Journal of Robotics and Control (JRC), vol. 4, no. 2, pp. 217-226, 2023.

[24] M. K. Saleem, M. L. U. R. Shahid, A. Nouman, H. Zaki, and M. A. U. R. Tariq, ““Design and implementation of adaptive neuro-fuzzy inference system for the control of an uncertain ball and beam apparatus,”“ Mehran University Research Journal Of Engineering & Technology, vol. 41, no. 2, pp. 178-184, 2022, DOI: 10.22581/muet1982.2202.17.”

[25] P. Chotikunnan, B. Panomruttanarug, N. Thongpance, M. Sangworasil, and T. Matsuura, ““An application of Fuzzy Logic Reinforcement Iterative Learning Control to Balance a Wheelchair,”“ International Journal of Applied Biomedical Engineering, vol. 10, no. 2, pp. 1–9, 2017.”

[26] R. Chotikunnan, P. Chotikunnan, A. Ma'arif, N. Thongpance, Y. Pititheeraphab, and A. Srisiriwat, ““Ball and Beam Control: Evaluating Type-1 and Interval Type-2 Fuzzy Techniques with Root Locus Optimization,”“ International Journal of Robotics and Control Systems, vol. 3, no. 2, pp. 286–303, 2023, doi: 10.31763/ijrcs.v3i2.997.”

[27] P. Rajesh, F. H. Shajin, V. Ansal, and V. K. B., “Enhanced artificial transgender longicorn algorithm & recurrent neural network based enhanced DC-DC converter for torque ripple minimization of BLDC motor,” Journal of Current Science and Technology, vol. 13, no. 2, pp. 182–204, 2023, doi: https://doi.org/10.59796/jcst.V13N2.2023.1735.

[28] D. Saputra, A. Ma'arif, H. Maghfiroh, P. Chotikunnan, and S. Rahmadhia, “Design and Application of PLC-based Speed Control for DC Motor

Using PID with Identification System and MATLAB Tuner," International Journal of Robotics and Control Systems, vol. 3, no. 2, pp. 233-244, 2023. doi: 10.31763/ijrcs.v3i2.775.

[29] P. Chotikunnan, R. Chotikunnan, and P. Minyong, "Adaptive Parallel Iterative Learning Control with A Time-Varying Sign Gain Approach Empowered by Expert System," Journal of Robotics and Control (JRC), vol. 5, no. 1, pp. 72-81, 2024. DOI: https://doi.org/10.18196/jrc.v5i1.20890.

[30] E. Widya Suseno and A. Ma'arif, "Tuning of PID Controller Parameters with Genetic Algorithm Method on DC Motor," International Journal of Robotics and Control Systems, vol. 1, no. 1, pp. 41-53, 2021. doi: 10.31763/ijrcs.v1i1.249.

[31] L. Fong, M. Islam, and M. Ahmad, "Optimized PID Controller of DC-DC Buck Converter based on Archimedes Optimization Algorithm," International Journal of Robotics and Control Systems, vol. 3, no. 4, pp. 658-672, 2023. doi: 10.31763/ijrcs.v3i4.1113.

[32] M. Khalifa, A. Amhedb, and M. Al Sharqawi, "Real Time DC Motor Position Control Using PID Controller in LabVIEW," Journal of Robotics and Control (JRC), vol. 2, no. 5, pp. 342-348, 2021. doi: 10.18196/jrc.25104.

[33] M. Samuel, M. Mohamad, M. Hussein, and S. Mad Saad, "Lane Keeping Maneuvers Using Proportional Integral Derivative (PID) and Model Predictive Control (MPC)," Journal of Robotics and Control (JRC), vol. 2, no. 2, pp. 78-82, 2021. doi: 10.18196/jrc.2256.

[34] E. Rahayu, A. Ma'arif, and A. Çakan, "Particle Swarm Optimization (PSO) Tuning of PID Control on DC Motor," International Journal of Robotics and Control Systems, vol. 2, no. 2, pp. 435-447, 2022. doi: 10.31763/ijrcs.v2i2.476.

[35] R. Kristiyono and W. Wiyono, "Autotuning Fuzzy PID Controller for Speed Control of BLDC Motor," Journal of Robotics and Control (JRC), vol. 2, no. 5, pp. 400-407, 2021. doi: 10.18196/jrc.25114.

[36] A. Baharuddin and M. Basri, "Self-Tuning PID Controller for Quadcopter using Fuzzy Logic," International Journal of Robotics and Control Systems, vol. 3, no. 4, pp. 728-748, 2023. doi: 10.31763/ijrcs.v3i4.1127.

[37] A. Saba, T. Sikiru, I. Bello, A. Salawudeen, and U. Dodo, "Modified Fractional Order PID Controller for Load Frequency Control of Four Area Thermal Power System," International Journal of Robotics and Control Systems, vol. 3, no. 2, pp. 187-205, 2023. doi: 10.31763/ijrcs.v3i2.957.

[38] M. Zadehbagheri, A. Ma'arif, R. Ildarabadi, M. Ansarifard, and I. Suwarno, "Design of Multivariate PID Controller for Power Networks Using GEA and PSO," Journal of Robotics and Control (JRC), vol. 4, no. 1, pp. 108-117, 2023. doi: 10.18196/jrc.v4i1.15682.

[39] A. Shuraiji and S. Shneen, "Fuzzy Logic Control and PID Controller for Brushless Permanent Magnetic Direct Current Motor: A Comparative Study," Journal of Robotics and Control (JRC), vol. 3, no. 6, pp. 762-768, 2022. doi: 10.18196/jrc.v3i6.15974.

[40] A. Wongkamhang, N. Wuttipan, R. Chotikunnan, K. Roongprasert, P. Chotikunnan, N. Thongpance, M. Sangworasil, A. Srisiriwat, et al., "Design and Develop a Non-Invasive Pulmonary Vibration Device for Secretion Drainage in Pediatric Patients with Pneumonia," Journal of Robotics and Control (JRC), vol. 4, no. 5, pp. 632-642, 2023. doi: 10.18196/jrc.v4i5.19588.

DOI: https://doi.org/10.15379/ijmst.v10i3.3393